14th International Conference on Structural Safety and Reliability - ICOSSAR'25
1-6 June, 2025 - Los Angeles California, USA
R. Ghanem, E. Johnson, S. Masri and A. Olivier (Eds)

DOES CLIMATE CHANGE CREATE MORE RISKS OR OPPORTUNITIES FOR OFFSHORE WIND ENERGY IN HURRICANE ZONES?

WEICHIANG PANG[1] AND SUSMITA BHOWMIK[2]

[1]Professor
Glenn Dept. of Civil Engineering, Clemson University, Clemson, SC
wpang@clemson.edu

[2]Graduate Student
Glenn Dept. of Civil Engineering, Clemson University, Clemson, SC
sbhowmi@g.clemson.edu

Key words: Hurricane, Climate Change, Risk, Opportunity, Offshore Wind Energy.

Abstract. This study introduces a statistical track simulation framework integrated with projected future climate data to assess the dual impact of climate change on offshore wind turbines (OWTs), namely, the potential increased risk of structural failure and the opportunity for enhanced power generation. Projections from the Shared Socio-economic Pathway SSP3-7.0 scenario are used to evaluate future wind conditions, turbine safety, and energy production potential. A Poisson regression model is used to simulate storm genesis, incorporating climate variables as predictors. Additionally, a probabilistic framework is developed to evaluate offshore wind turbine performance under wind hazards, using site-specific wind conditions to estimate the probability of failure. The results reveal that northeastern sites, such as those in Massachusetts and New York, may experience higher wind speeds in year 2060 than historical levels. This increase suggests greater energy generation potential, particularly during tropical cyclones that weaken upon reaching these areas. These weaken storms often produce strong wind but non-destructive winds, offering northeastern sites an opportunity to harness more wind energy under future climate scenarios. In contrast, results highlight that designing for the current climate but evaluating under future (SSP3-7.0) hazards leads to a rise in failure risk. By examining both the risks and opportunities, this research highlights the importance of region-specific strategies to optimize offshore wind energy deployment in a changing climate.

1 INTRODUCTION

Offshore wind energy is a renewable resource with significant growth potential, particularly in the United States (U.S.). In 2020, the total installed wind capacity globally was 745 GW [1], while the U.S. alone contributed 135.843 GW [2]. The U.S. aims to expand offshore wind energy, targeting 30 GW by 2030 and 110 GW by 2050 [3]. As of April 2025, the U.S. Bureau of Ocean Energy Management (BOEM) has designated numerous areas for offshore wind development, including Wind Energy Areas (WEAs), lease areas, and call areas. These

designations span various regions of the U.S. Outer Continental Shelf (OCS), such as the Atlantic Coast, the Gulf of Mexico, the Pacific Coast, and the Gulf of Maine [4]. While offshore wind energy presents significant opportunities for expanding clean energy production, many of these areas are vulnerable to hurricane impacts. Offshore wind turbines in hurricane-prone regions face risks such as extreme wind loads, wave impacts, and potential structural failures during severe tropical cyclones [5]. These risks are further amplified by climate change, which is projected to increase the intensity and frequency of major hurricanes. It may pose additional challenges to the long-term reliability and safety of offshore wind infrastructure.

Previous studies have developed different methods to create a stochastic simulation of hurricanes by simulating the frequency, intensity, and track of hurricane storms based on historical data ([6],[7]). As the formulation of hurricanes depends heavily on climate conditions, climate changes will impact the frequency, intensity, and track of hurricanes. Based on historical data from the North Atlantic Ocean, previous studies have demonstrated a positive correlation between sea surface temperature (SST) and the frequency and intensity of tropical cyclones ([8],[9]). In addition, the Poisson regression model is widely used to simulate storm genesis by incorporating climate variables such as sea surface temperature (SST), relative humidity (RH), vertical wind shear (VWS), absolute vorticity (VO), and storm location through statistical approaches ([10],[11]). Thus, this study explores the effects of rising SST due to climate change on tropical cyclones, focusing on their impact on the risks and opportunities for offshore wind energy production.

2 SIMULATION FRAMEWORK

This study generates synthetic hurricane tracks using a stochastic simulation framework originally proposed in [12], as illustrated in Figure 1. The state of the storms and the simulation procedure are described in previous studies ([6],[13]). This study uses two simulation models: (1) a baseline model, which keeps current sea surface temperatures (SST) level in the intensity model, and (2) a climate change model, which incorporates SSTs from SSP3-7.0 scenarios for the year 2060 in the intensity model and also, new annual storms frequency using SSTs, relative humidity (RH), and wind shear (WS) from SSP3-7.0 scenarios for the year 2060 to investigate the climate change effects on OWTs.

2.1 Hurricane simulation model and climate change effects

The simulation model consists of several modules: the hurricane genesis model, tracking model, intensity (central pressure) model, central pressure decay (filling rate) model, wind field model, and boundary layer model. The simulation uses hurricane records from the HURDAT2 database [14] from the start of satellite observations (1966) to 2021.

In this study, the Global climate model (GCM), CESM2 (USA) from the Coupled Model Intercomparison Project Phase 6 (CMIP6) data repository [15] is used in the climate change model. A total of 16 GCMs are chosen based on the High-Resolution Model Intercomparison Project (HighResMIP) and Scenario Model Intercomparison Project (ScenarioMIP) parts of CMIP6, data availability, and models considered in previous studies. CESM2 is selected after assessing the performance of each GCM using weighted SST errors and calculating the difference between SSTs from model and observation data. Figure 2 shows the monthly averaged SST for September, while Figure 3 illustrates the difference in SST between observed

and GCM-simulated values for the year 2020. The simulated sea surface temperatures (SSTs) from the GCM reveal systematic biases. Therefore, implementing bias correction on these SSTs

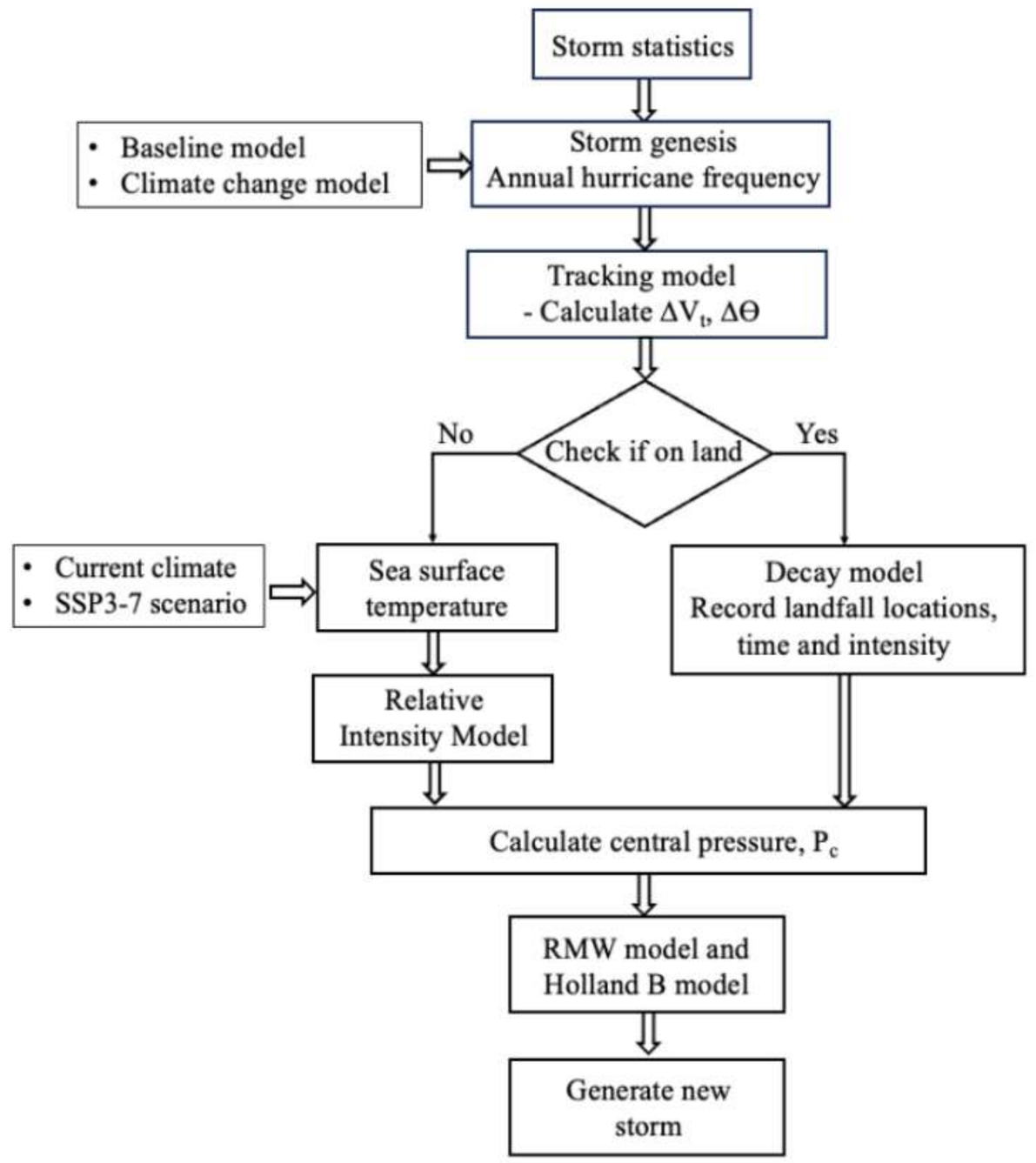

Figure 1: Hurricane simulation framework.

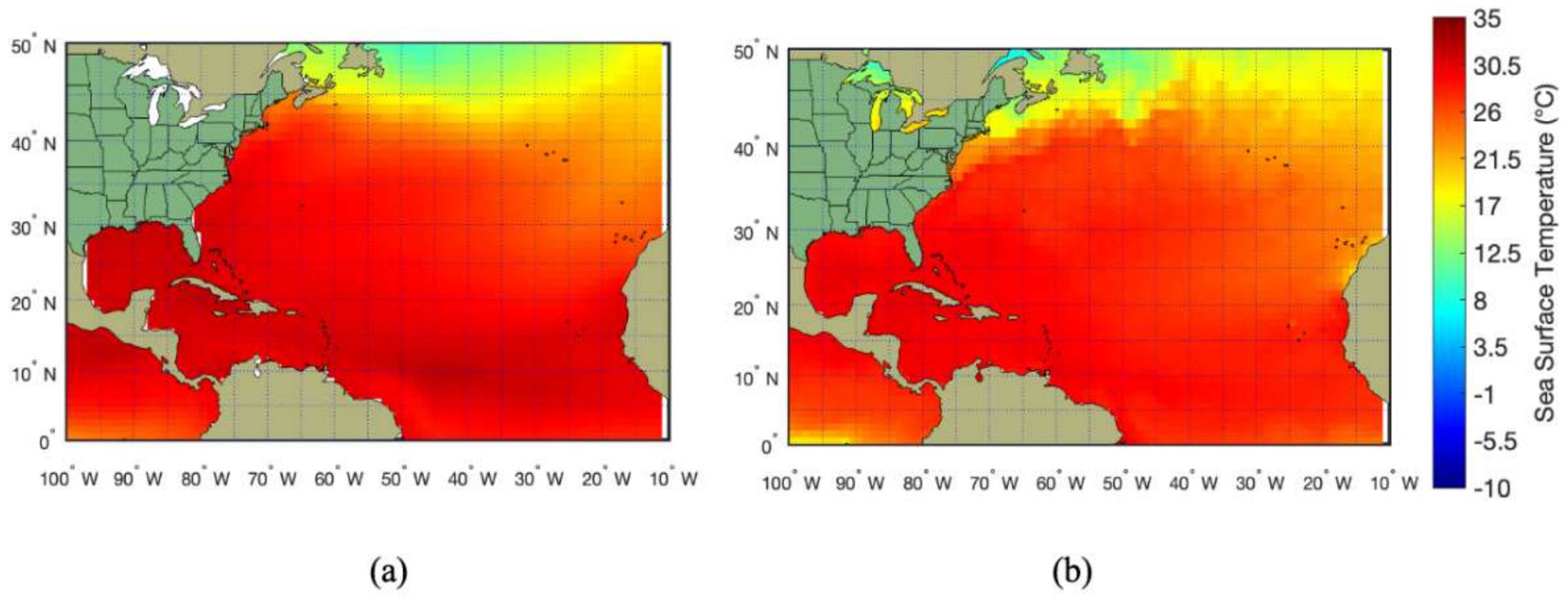

Figure 2: Monthly averaged sea surface temperature (SST) for September (a) SSP3-7.0 scenario for year 2060 (CESM2); (b) observation for year 2020 (ERA5);

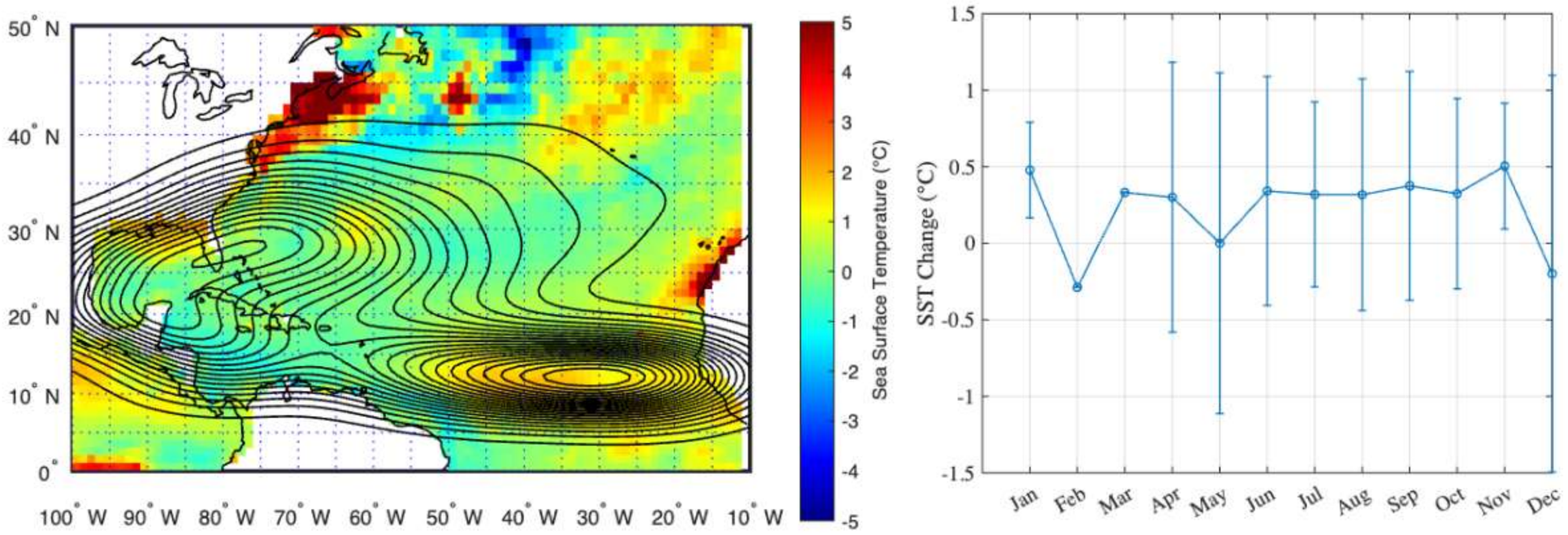

(a) (b)

Figure 3: Changes in monthly averaged sea surface temperature (SST) [2020 from (SSP3-7.0) minus 2020 observations (ERA5)] based on the CESM2 model: (a) for September; (b) for all months (mean ± standard deviation).

is essential to enhance the accuracy of future projections. Kernel density estimation (KDE) contours are used in Figure 3 to show the historical storm spawn locations from 1851 to 2021. However, this study uses the as-simulated outputs from the CESM2 model to obtain the preliminary results.

2.2 Genesis model

In the baseline model, the annual number of storms recorded in HURDAT2 is fitted to a negative binomial distribution, with parameters R and P estimated using maximum likelihood methods. The mean annual storm frequency is 16.82 storms/year, and the standard deviation is 5.12 storms/year based on historical storm data from 1966 to 2021. The probability mass function of the distribution is given in Equation (1), where the random variable x represents the number of storms in a year:

$$f(x) = \binom{x + R - 1}{x} P^R (1 - P)^x \tag{1}$$

The annual number of storms in baseline model is randomly selected from the negative binomial distribution fit using historical data.

The Poisson regression equation [10] is used to investigate the influence of climate change on genesis activity. In regression, the expected number of hurricanes per month for each 5^0 by 5^0 grid cell, μ, can be modeled as a linear pattern of predictor variables, T_s, RH, WS, VO, ϕ , which represents grid-averaged monthly mean relative SST, RH at 600 hPa, VWS between the 850 and 200 hPa levels, relative vorticity at 850 hPa, and initial storm location, respectively. The new mean annual storm frequency is 20.01 storms/year, and the standard deviation is 4.46 storms/year using climate variables for 2060 from CESM2 (USA).

$$\mu = exp\,(\beta_0 + \beta_1 T_s + \beta_2 RH + \beta_3 WS + \beta_4 VO + log cos\phi) \tag{2}$$

Where, β_0 is constant and β_1 to β_4 are the coefficients which are obtained by using least square regression method.

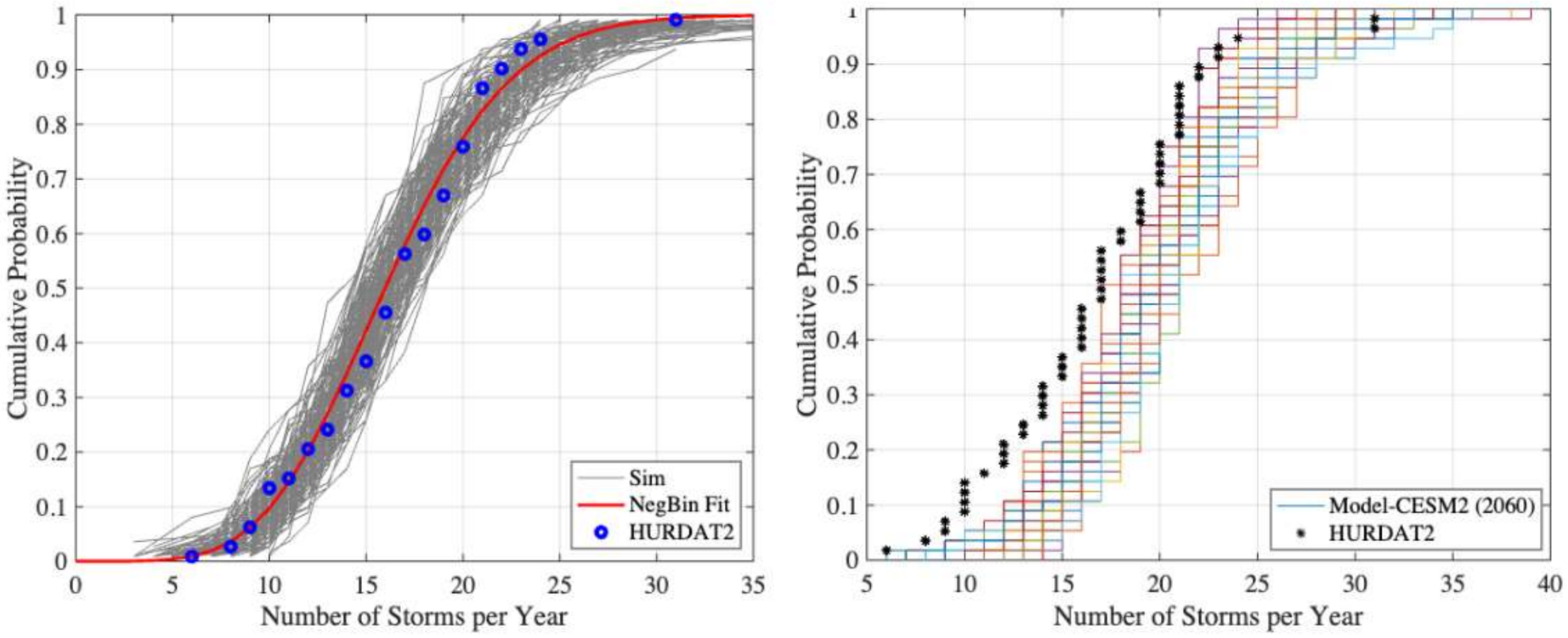

Figure 4: Cumulative distribution functions of observed and simulated annual spawn rates using (a) baseline genesis model; (b) climate change genesis model.

2.3 Site selection

Wind hazard curves are developed for eleven offshore wind sites, as shown in Figure 5. These include (1) six sites within active lease areas along the US East Coast, Vineyard Wind (MA), Equinor (NY), Atlantic Shores Offshore Wind (NJ), US Wind (MD), Coastal Virginia Offshore Wind Pilot (VA), and Kitty Hawk (NC); (2) two sites from proposed lease areas, South Carolina (SC) and Texas (TX); and (3) three hypothetical shallow-water sites near Florida, FL1, FL2, and FL3. These locations are selected to support the reliability and uncertainty analysis by capturing a range of wind climate conditions across the Atlantic and Gulf of Mexico Outer Continental Shelf.

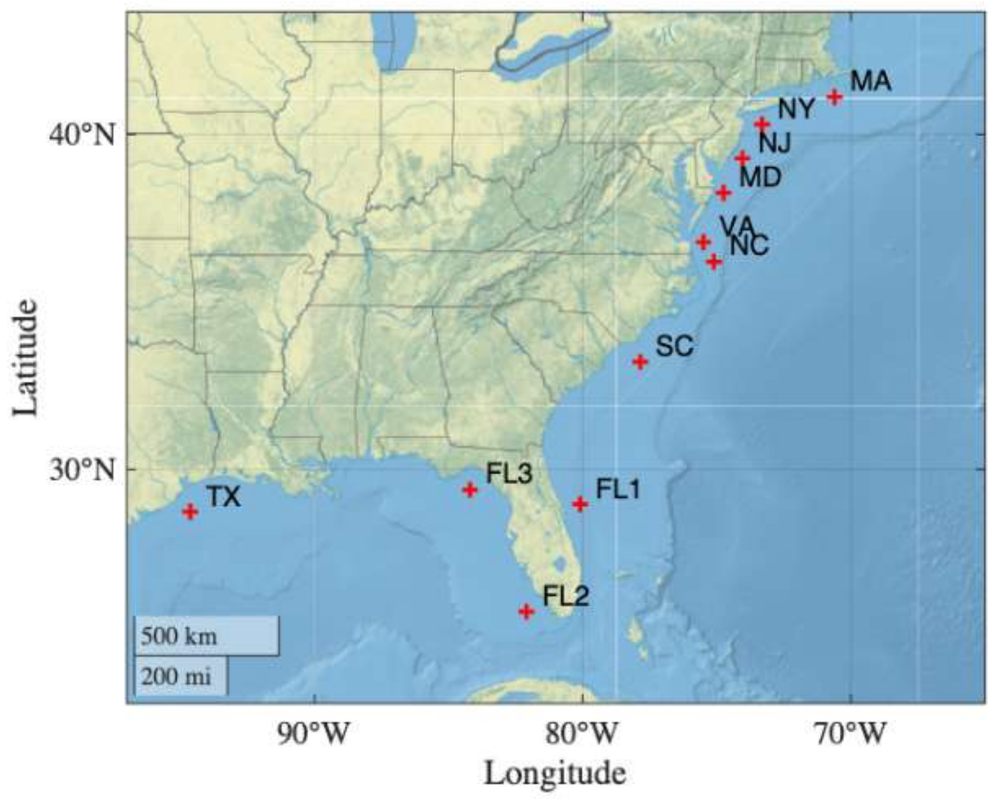

Figure 5: Locations of shallow water offshore wind energy sites.

2.4 Risk and opportunity metrics

In this study, the NREL 5-MW reference turbine [16] is used to evaluate offshore wind energy performance under wind-induced hazard conditions. Wind turbines are typically designed for an operational lifespan between 20 and 30 years [17]. In this study, a target lifespan of 25 years is assumed for performance evaluation.

To assess the risks and opportunities associated with climate change, three key metrics are used:

(1) the wind hazard curve, representing peak wind speed versus mean return period (RP)
(2) the change in mean annual power generation (expressed as net gain/loss in kW-hr)
(3) the mean annual probability of tower failure (expressed as reliability index).

For Metric 1, wind speeds at a given site are estimated by selecting events from the 10,000-year simulated hurricane catalog that pass within a 500 km radius of the location. This selection radius is chosen to efficiently capture significant storm influences while minimizing computational demand. Events beyond 500 km are assumed to have little or no impact on wind speeds at the site.

The performance of the NREL 5-MW wind turbine is defined by its power curve (Figure 6), which shows how wind speed affects power output. The turbine starts rotating and generating power at a cut-in speed of 3 m/s and stops at a cut-out speed of 25 m/s to avoid damage. In this study, it is assumed that power generation ceases when wind speeds at hub height reach or exceed 25 m/s. The net power gain or loss (Metric 2) is evaluated by calculating the difference between the mean annual energy output (E_I) and the baseline energy production.

The baseline energy production is estimated using the following equation:

$$E_{base} = CF \times G(V_{max}) \times t_j \tag{3}$$

Where, *CF* is the capacity factor for each site, obtained from the Global Wind Atlas [18]; $G(V_{max})$ is the maximum power output of the turbine, t_j is the storm duration when wind speeds exceed the average wind speed. The average wind speed is derived from the power generation curve, which is determined based on actual generated power. The actual generated power is calculated as the product of the capacity factor and the maximum power output.

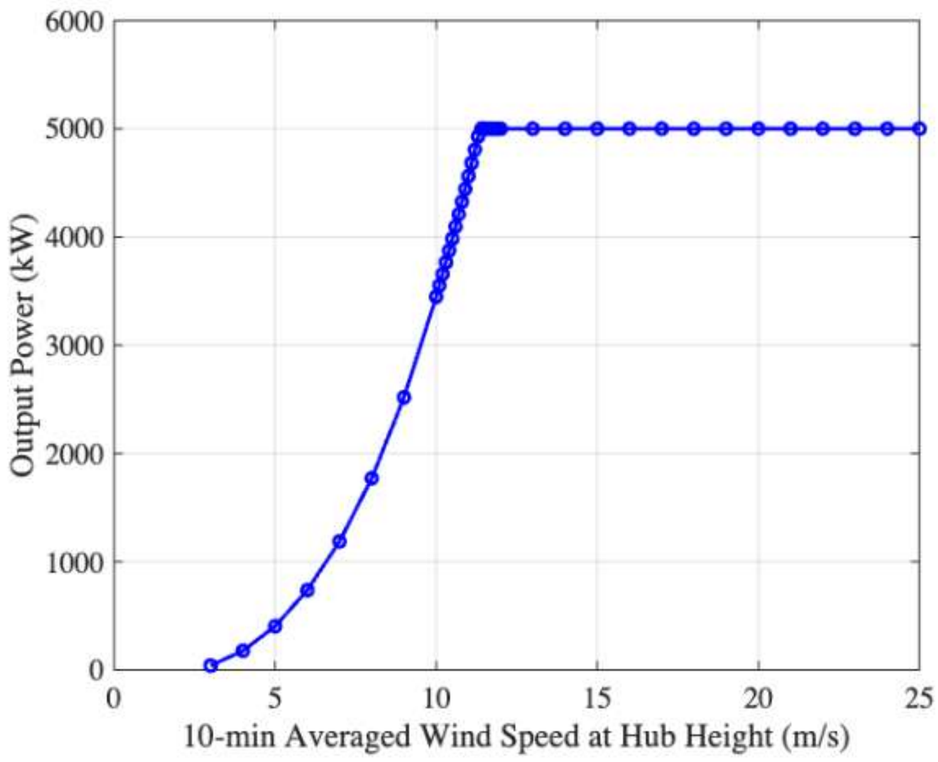

Figure 6: Power generation curve of the NREL 5-MW wind turbine.

The mean annual power generation for one wind turbine from the wind energy of tropical cyclones (E_1) is computed using the following equation:

$$E_1 = \frac{\sum_{i=1}^{i=N} \int_{t=t_o}^{t=t_{end}} G\big(V_i(t)\big)dt}{Y_{sim}} \tag{4}$$

Where, $V_i(t)$ is the hub height wind speed time history during the passage of the *i-th* tropical cyclone within 500 km from the wind turbine; $G(.)$ is the power curve function; Y_{sim} is the total simulation years; to is the starting time step; t_{end} is the ending time step; N is the total number of tropical cyclones in 10,000 years, that pass within 500 km of the wind turbine.

The mean annual tower failure probability (Metric 3), P_{f1}, is used to quantify the risk of tropical cyclones.

$$P_{f1}(v) = \int_{v=0}^{v=\infty} P_{e1}(v) \times F_r(v, T_c)dv \tag{5}$$

Where, $P_{f1}(v)$ is the site-specific annual exceedance probability of wind speed and $F_r(v, T_c)$ is the tower buckling fragility curve defined as a function of thrust capacity and wind speed. The tower buckling fragility curve is expressed as:

$$F_r(T_C < T_D | \, v) = 1 - \Phi\left(\frac{\psi_C - \psi_D(v)}{\sqrt{\xi_C^2 + (\xi_D(v))^2}}\right) \tag{6}$$

where $F_r(T_C < T_D | \, v)$ is the probability of tower buckling failure defined in terms of thrust capacity , T_c and thrust demand, T_D at a given wind speed, v. ψ_C is the logarithmic mean of thrust capacity and ψ_D is the logarithmic mean of thrust demand as a function of wind speed. ξ_C is the logarithmic standard deviation of thrust capacity and ξ_D is the logarithmic standard deviation of thrust demand as a function of wind speed. In this study, ξ_C is considered as 0.15 based on material and geometric uncertainty.

The annual failure probability is calculated for the dominant load case (DLC 6.2) by convolving the fragility curve with a site-specific hazard curve (Equation 5). The as-designed fragility curves are generated for two yaw configurations: 0^0 yaw and 65° yaw. It is observed that the maximum thrust occurs at a 65° yaw error. The demand parameters for the 0° yaw configuration are computed using the equation $y = 0.0754x^{1.8877}$, while those for the 65^0 yaw configuration are from the equation $y = 0.2626x^2$.

Four distinct scenarios are analyzed to compute the annual probability of failure: (1) Case 1 (D_{cc} and H_{cc}): The design is based on the maximum wind speeds for each event under the current climate, and the site-specific hazard curve corresponds to the current climate conditions. (2) Case 2 (D_{cc} and H_{SSP}): The design is based on the maximum wind speeds for each event under the current climate, while the site-specific hazard curve corresponds to the projected climate conditions for the year 2060. (3) Case 3 (D_{SSP} and H_{cc}): The design is based on the maximum wind speeds for each event under the projected climate conditions in 2060, while the site-specific hazard curve corresponds to the current climate conditions. (4) Case 4 (D_{SSP} and H_{SSP}): The design is based on the maximum wind speeds for each event under the projected climate conditions for 2060, and the site-specific hazard curve also corresponds to the projected climate conditions for 2060.

3 RELIABILITY AND UNCERTAINTY ANALYSIS

3.1 Wind hazard

As per the IEC 61400-1 standard [19], the structural design of wind turbines is based on the 10-minute average wind speeds at hub height, considering return periods of 50 and 500 years. Figure 7 illustrates the hurricane wind hazard curves for both the current climate and the projected climate scenario SSP3-7.0 for the year 2060 across eleven wind turbine locations. The findings indicate a notable rise in design wind speeds for future scenarios due to climate change. For instance, at the MA site, there is an approximate 46% increase in peak wind speed for the future scenario SSP3-7.0 (CESM2 (USA)) with a 50-year return period and a 34% increase for a 500-year return period. Table 1 presents the peak wind speeds for all eleven sites for both 50- and 500-year return periods, along with the differences between current and future climate conditions.

3.2 Power generation change

The distribution of the power generation across the 10,000-year database of hurricane storms gave an indication of the variability in power generation due to hurricanes. An example of this variability is shown in Figure 8 for the Massachusetts site (MA), which compares the power generation for years where the power generation was non-zero (i.e., at least one storm passed within 500 km of the site). The annual power generation change (net gain) from tropical cyclone-induced winds of each of the eleven analyzed sites is described in Figure 9. As expected, the highest power generation (net gain) was predicted at the sites that are largely considered the most susceptible to hurricanes (North Carolina, South Carolina and Florida). Additionally, the change in power production, considering the increase in sea-surface temperature due to climate change, is most significant for states further north (Massachusetts, New York, New Jersey, and Maryland), at as much as 50%. The sites further south and in the Western Gulf Coast show a decline in power generation under future sea-surface temperature conditions, indicating that climate change may reduce wind energy potential in these regions compared to the current climate.

3.3 Probability of failure

In this study, the structural capacity was assessed based on ULS, with results presented for DLC 6.2, representing one of the ultimate design's critical loading scenarios. It is important to note that wind turbine towers are typically designed by fatigue considerations rather than ultimate limit state (ULS) criteria, with critical sections often operating at less than 50% utilization. The annual probability of failures is converted into a reliability index for better visualization. Figure 10 illustrates the annual reliability index for each site, corresponding to 0° yaw error and 65° yaw error, respectively.

The findings reveal a detectable increase in the likelihood of failure across all sites when accounting for a changing climate. Notably, if the tower is designed for the current climate and evaluated using the current climate hazard curve, or if it is designed for the future scenario (SSP3-7.0 for the year 2060) and evaluated using the future hazard curve, both scenarios yield similar annual probabilities of failure for 65° yaw error. However, if the tower is designed for the current climate but evaluated using the future hazard curve, the annual probability of failure

increases substantially. Conversely, if the tower is designed for the future climate but evaluated using the current hazard curve, the annual probability of failure is significantly lower.

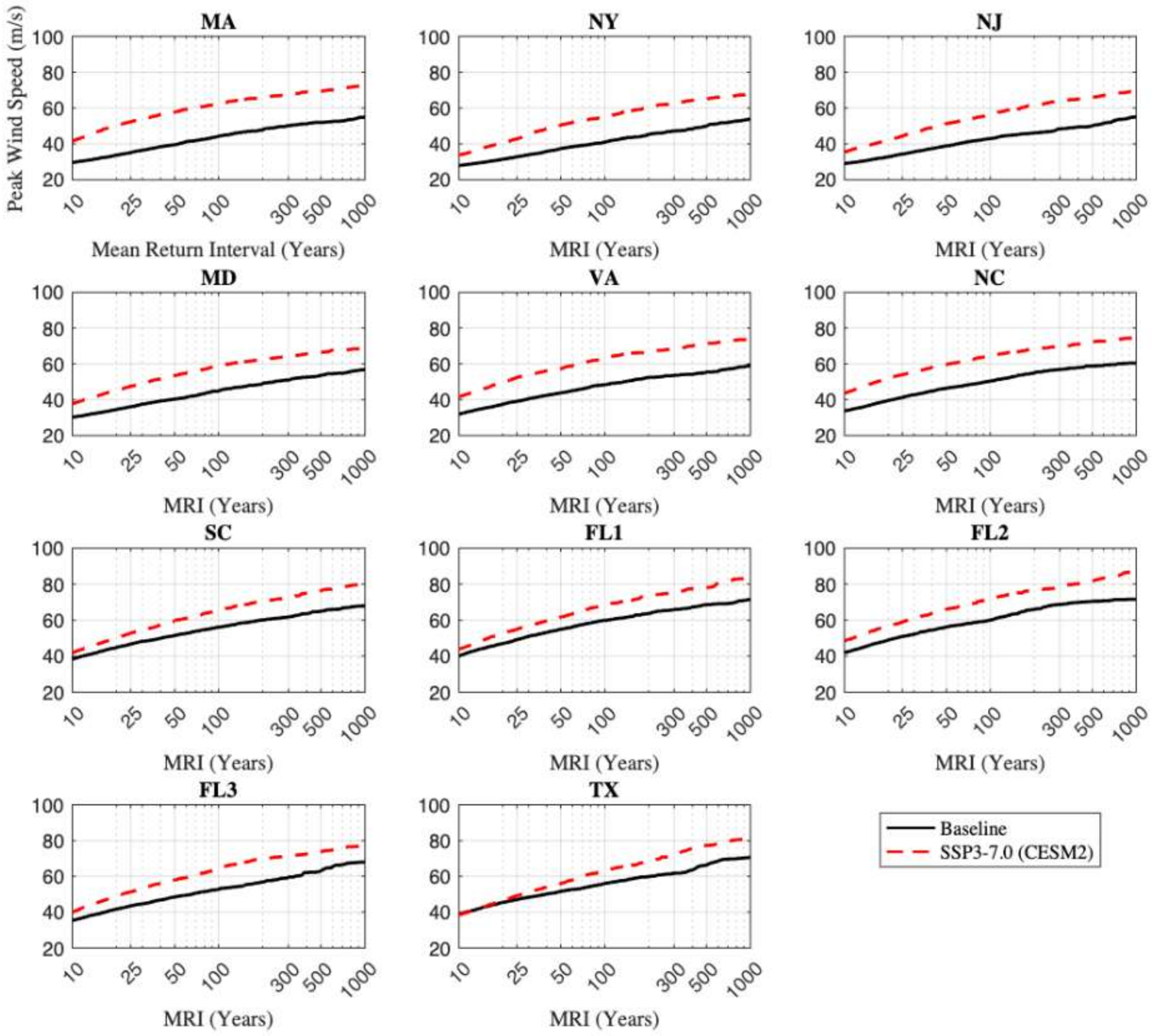

Figure 7: 10min averaged peak wind speed at hub height (90m) versus mean return interval for each of the offshore wind energy sites under current climate (baseline) and year 2060 SSP3-7.0 climate (CESM2).

Table 1: Peak wind speeds for all eleven sites (m/s)

Site	50-Year RP			500-Year RP		
	Baseline	SSP3-7.0	% Difference	Baseline	SSP3-7.0	% Difference
MA	39.5	57.8	46	52.0	69.6	34
NY	37.4	50.5	35	49.9	64.9	30
NJ	38.9	51.3	32	50.1	66.0	32
MD	40.4	53.5	32	53.6	66.4	24
VA	43.8	57.3	31	55.4	71.4	29
NC	46.4	59.8	29	58.9	72.0	22
SC	51.5	59.7	16	65.0	76.3	17
FL1	55.0	61.6	12	68.5	78.2	14
FL2	56.2	66.1	18	70.4	81.6	16
FL3	48.5	58.0	20	63.0	73.6	17
TX	51.7	55.9	8	66.3	77.3	17

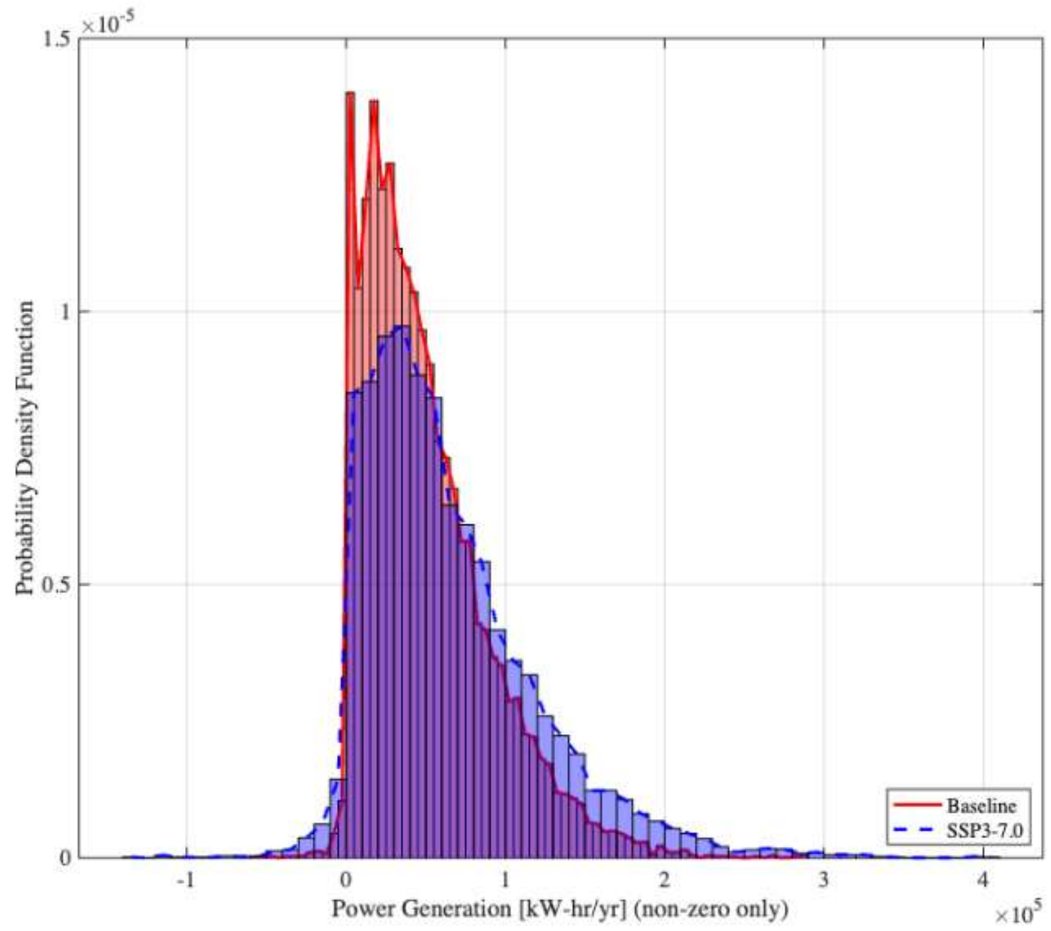

Figure 8: Distribution of 10,000 years of simulated annual power generation for MA site from tropical cyclone winds under the current climate and the 2060 SSP3-7.0 climate.

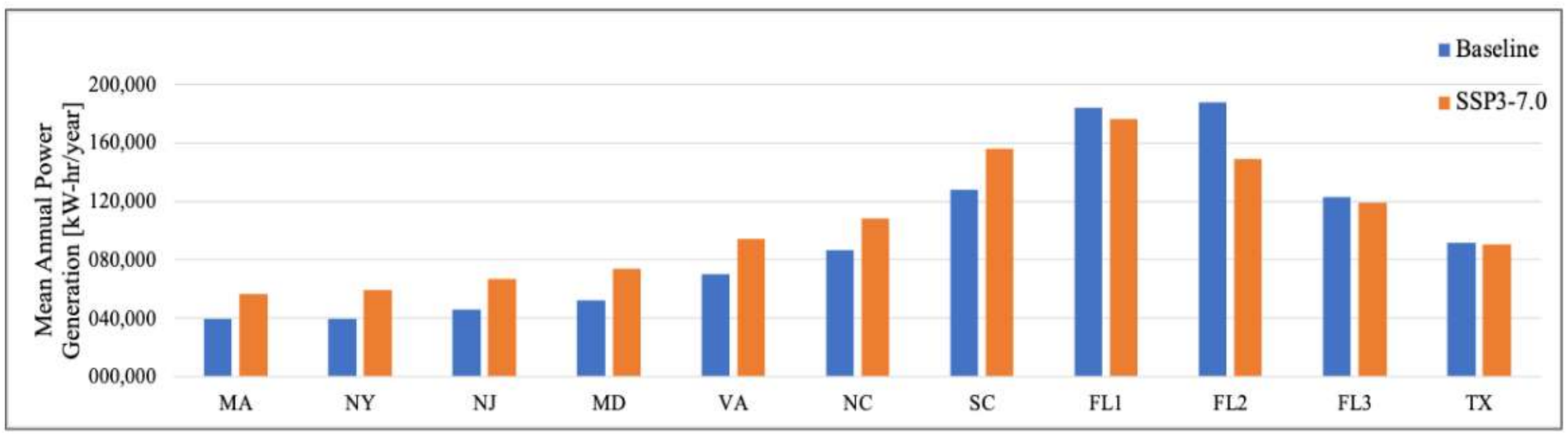

Figure 9: Mean annual power generation due to tropical cyclone wind for one NREL 5MW turbine at each of the sites.

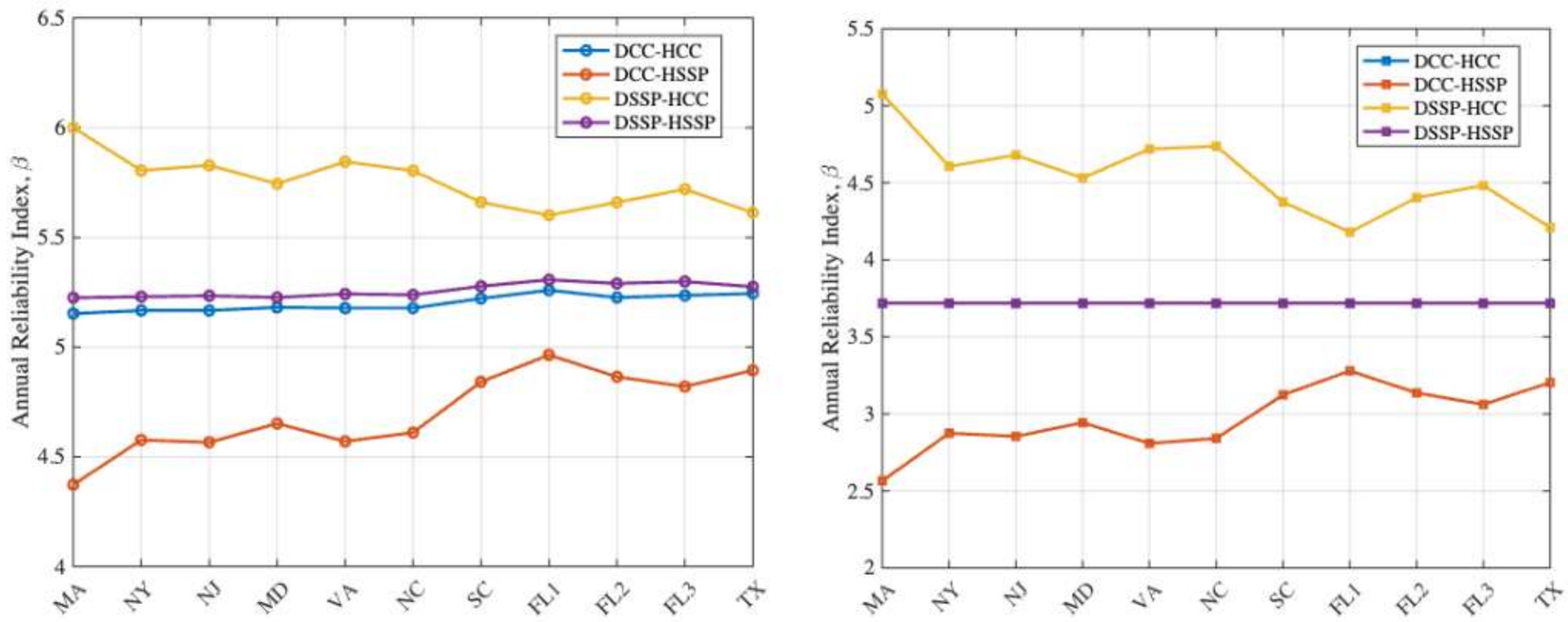

Figure 10: Annual reliability index for wind at each of the sites at (a) 0° yaw error; (b) 65° yaw error.

4 CONCLUDING REMARKS

This study presents a framework to evaluate the impacts of climate change on offshore wind turbines, specifically examining how rising sea surface temperatures influence offshore wind energy production, considering both risks and opportunities. The analysis focuses on the significant wind loads generated by hurricanes on offshore wind turbines with fixed bottom support structures, while wave loads are not considered.

The results show a notable increase in wind speeds at the examined wind turbine sites by the year 2060, attributed to elevated sea surface temperatures. In this study, the as-projected climate outputs from a global climate model (GCM) were used to derive preliminary results. A comparison between the model projected and observed sea surface temperatures for the year 2020 revealed biases exist in the model. Future analyses will incorporate bias correction techniques to improve the accuracy of climate projections and produce more representative outcomes.

In assessing the benefits, it was found that the greatest potential for additional power generation from wind and the energy of non-direct hits from tropical cyclones lies in regions with a higher frequency of hurricanes, such as North Carolina, South Carolina, and Florida. Furthermore, the impact of rising sea surface temperatures on additional power generation from tropical cyclones is most pronounced in northern states, including Massachusetts, New York, New Jersey, and Maryland, where increases of up to 50% may be observed when compared to current climate.

This study evaluates hurricane-related risks to offshore wind turbines at each location by integrating fragility curves with site-specific hazard data. Results show that designing turbines for current climate conditions but subjecting them to future hazards notably increases the risk of structural failure. In contrast, designing for future climate conditions enhances structural reliability, even when evaluated under present-day hazards. These findings underscore the importance of incorporating future climate projections into offshore wind turbine design to ensure long-term structural performance and reliability.

5 ACKNOWLEDGEMENTS

The authors gratefully acknowledge the partial support of the National Offshore Wind Research & Development Consortium (NOWRDC) and the technical support of Palmetto Cluster at Clemson University.

REFERENCES

[1] Share of Electricity Production fromWind, (n.d.) OurWorld in Data. Available online: https://ourworldindata.org/grapher/share-electricity-wind (accessed on 1 December 2022). U.S. Department of Energy. (2023).

[2] Wikipedia. Wind Power in the United States. Available online: https://en.wikipedia.org/wiki/Wind_power_in_the_United_States (accessed on 19 December 2022).

[3] Musial, W., Beiter, P., Schwabe, P., Tian, T., Stehly, T., and Spitsen P. *Offshore Wind Technologies Market Report*, U.S. Department of Energy, Washington DC (2022).

[4] U.S. Bureau of Ocean Energy Management (BOEM), "Wind Planning Areas," (2025). [Online]. Available: [https://www.boem.gov/oil-gas-energy/wind-planning-areas].

[5] Hallowell, S. T., Myers, A. T., Arwade, S. R., Pang, W., Rawal, P., Hines, E. M., ... and Fontana, C. M. Hurricane risk assessment of offshore wind turbines. *Renewable Energy*, (2018) 125, 234-249.

[6] Liu, F., and Pang, W. Influence of climate change on future hurricane wind hazards along the US eastern coast and the Gulf of Mexico. *In Advances in Hurricane Engineering: Learning from Our Past* (pp. 573-584) (2013).

[7] Cui, W., and Caracoglia, L. A new stochastic formulation for synthetic hurricane simulation over the North Atlantic Ocean. *Engineering Structures*, 199, 109597 (2019).

[8] Mudd, L., Wang, Y., Letchford, C., and Rosowsky, D. Assessing climate change impact on the US East Coast hurricane hazard: temperature, frequency, and track. *Natural Hazards Review*, (2014) 15(3), 04014001.

[9] Knutson, T. R., Chung, M. V., Vecchi, G., Sun, J., Hsieh, T. L., and Smith, A. J. Climate change is probably increasing the intensity of tropical cyclones. *Tyndall Centre for Climate Change Research* (2021).

[10] Tippett, M. K., Camargo, S. J., and Sobel, A. H. A Poisson regression index for tropical cyclone genesis and the role of large-scale vorticity in genesis. *Journal of Climate*, (2011) 24(9), 2335-2357.

[11] Lee, C. Y., Tippett, M. K., Sobel, A. H., and Camargo, S. J. An environmentally forced tropical cyclone hazard model. *Journal of Advances in Modeling Earth Systems*, (2018) 10(1), 223-241.

[12] Vickery, P. J., Skerlj, P. F., and Twisdale, L. A. Simulation of hurricane risk in the US using empirical track model. *Journal of structural engineering*, (2000) 126(10), 1222-1237.

[13] Bhowmik, S., Pang, W., and Stoner, M. Probabilistic modeling of North Atlantic Ocean hurricane spawn considering climate change. In Proceedings of the *14th International Conference on Applications of Statistics and Probability in Civil Engineering*, ICASP14, Dublin, Ireland (2023).

[14] Landsea, C. W., and Franklin, J. L. Atlantic hurricane database uncertainty and presentation of a new database format. *Monthly Weather Review*, (2013) 141(10), 3576-3592.

[15] Copernicus Climate Change Service, Climate Data Store, (2021): CMIP6 climate projections. Copernicus Climate Change Service (C3S) Climate Data Store (CDS). DOI: 10.24381/cds.c866074c (Accessed on 16-Nov-2023).

[16] Jonkman, J., Butterfield, S., Musial, W., and Scott, G. Definition of a 5-MW reference wind turbine for offshore system development (No. NREL/TP-500-38060). National Renewable Energy Lab. (NREL), Golden, CO (United States) (2009).

[17] Wiser, R. H., and Bolinger, M. Benchmarking anticipated wind project lifetimes: Results from a survey of US wind industry professionals (2019).

[18] Davis, N. N., Badger, J., Hahmann, A. N., Hansen, B. O., Mortensen, N. G., Kelly, M., ... and Drummond, R. The Global Wind Atlas: A high-resolution dataset of climatologies and associated web-based application. *Bulletin of the American Meteorological Society*, (2023) 104(8), E1507-E1525.

[19] International Electrotechnical Commission (IEC). Wind energy generation systems - Part 3-1: Design requirements for fixed offshore wind turbines. IEC 61400-3-1. ISBN 978-2-8322-7609-9 (2019).